Check for updates

https://doi.org/10.4047/jap.2026.18.2.145

Differential effects of abutment contamination within an internal hexagonal connection on preload formation and load-dependent preload loss

Minji Sun[1], Jihoon Shin[2], Yeseul Park[2], June Sung Shim[3], Jaeyoung Kim[3]*

[1]Department of Prosthodontics, Ewha Womans University, Seoul, Republic of Korea
[2]Department of Prosthodontics, Oral Science Research Center, Yonsei University College of Dentistry, Seoul, Republic of Korea
[3]Department of Prosthodontics, Yonsei University College of Dentistry, Seoul, Republic of Korea

ORCID
Minji Sun
https://orcid.org/0000-0002-7402-2128
Jihoon Shin
https://orcid.org/0009-0009-4797-4869
Yeseul Park
https://orcid.org/0009-0003-6630-4058
June Sung Shim
https://orcid.org/0000-0003-1428-0122
Jaeyoung Kim
https://orcid.org/0000-0002-2412-891X

Corresponding author
Jaeyoung Kim
Department of Prosthodontics, Yonsei University College of Dentistry, 50-1 Yonsei-ro, Seodaemun-gu, Seoul 03722, Republic of Korea
Tel +82222283160
E-mail jaeyoungkim@yuhs.ac

Received December 29, 2025 / **Last Revision** February 8, 2026 / **Accepted** February 24, 2026

This research was supported by the Yonsei University College of Dentistry Fund (6-2022-0010).

PURPOSE. The purpose of this *in vitro* study was to quantitatively evaluate the effect of surface contamination within an internal hexagonal implant-abutment connection on preload formation and preload loss under cyclic loading conditions. **MATERIALS AND METHODS.** Internal hexagonal implant-abutment assemblies were divided into three groups according to the degree of surface contamination: no contamination (CT0), partial contamination (CT3), and extensive contamination (CT6). Reverse torque values were measured after initial tightening to assess preload formation (pre-RTV). Specimens were then subjected to cyclic loading, after which post-loading reverse torque values were recorded (post-RTV), and absolute torque loss (ΔRTV) was calculated. Surface alterations were qualitatively assessed using scanning electron microscopy (SEM). Statistical analyses were performed to compare torque-related outcomes among groups. **RESULTS.** Pre-RTV were significantly lower in the contaminated groups than in the uncontaminated control ($P < .001$), with no significant difference between CT3 and CT6. After cyclic loading, post-RTV decreased progressively with increasing contamination ($P < .001$). ΔRTV was significantly greater in CT6 than in CT0 and CT3 ($P < .001$), whereas no significant difference was observed between CT0 and CT3. SEM revealed localized surface wear at line angles in contaminated specimens, whereas uncontaminated specimens exhibited minimal surface alteration. **CONCLUSION.** Surface contamination within an internal hexagonal implant–abutment connection adversely affects joint stability through two distinct mechanical stages. While the presence of contamination primarily compromises initial preload formation, extensive contamination accelerates preload loss under cyclic loading. These findings suggest that even subtle contamination, often overlooked clinically, may have meaningful implications for implant-abutment stability. [J Adv Prosthodont 2026;18:145-54]

KEYWORDS

Loosening mechanism; Surface contamination; Screw loosening; Reverse torque value

© 2026 The Korean Academy of Prosthodontics
This is an Open Access article distributed under the terms of the Creative Commons Attribution Non-Commercial License (https://creativecommons.org/licenses/by-nc/4.0) which permits unrestricted non-commercial use, distribution, and reproduction in any medium, provided the original work is properly cited.

 https://doi.org/10.4047/jap.2026.18.2.145

INTRODUCTION

Abutment screw loosening remains one of the most common mechanical complications in implant prosthodontics.[1,2] Despite the high long-term survival rates of dental implants, screw loosening continues to compromise prosthesis stability, increase maintenance requirements, and necessitate repeated clinical interventions.[3-7] Consequently, this complication has persisted as a clinically relevant issue in both daily practice and prosthodontic research.

To date, efforts to reduce abutment screw loosening have focused primarily on mechanical optimization under contamination-free conditions. These investigations have addressed factors such as implant-abutment connection design, abutment screw geometry and material properties, and surface treatments intended to improve preload and reduce frictional loss.[8-17] Although these studies have substantially contributed to understanding screw joint mechanics, they were conducted primarily under idealized experimental conditions that do not fully reflect contemporary clinical workflows.

As mechanical configurations became more established, research interest gradually shifted toward reproducing contamination-related clinical conditions. Several studies have attempted to simulate contamination with saliva, blood, or other foreign substances to evaluate their effects on screw loosening.[18-20] However, in most of these investigations, contamination was applied primarily to the abutment screw. Because abutment screws can be readily replaced or segregated between laboratory and clinical use, screw contamination is generally considered a manageable factor in routine prosthodontic practice.

In contrast, contamination of the abutment itself presents a different clinical challenge. Custom abutments are most often fabricated in external dental laboratories using CAD-CAM workflows and are exposed to multiple potential sources of contamination during milling, finishing, and handling procedures (Fig. 1). Furthermore, prosthetic fabrication procedures are frequently performed directly on the same abutment, increasing the likelihood of cumulative contamination.[21-23] Unlike abutment screws, contaminated abutments cannot be readily replaced in clinical practice and are often delivered and used without thorough inspection or decontamination.

Despite its clinical relevance, abutment contamination within an internal hexagonal implant connection has received limited focused investigation. In internal connection implant systems, the hexagonal portion of the abutment presents flat surfaces that are commonly assumed to allow straightforward visual inspection and cleaning. Consequently, contamination in this area is often perceived as easily manageable and tends to receive limited attention during routine clinical procedures. However, such assumptions may contribute to inadvertent oversight, and the mechanical implications of abutment surface contamination, particularly in relation to screw-loosening mechanisms at the implant-abutment interface, remain insufficiently elucidated.

Therefore, the purpose of this study was to conduct a quantitative assessment of the effect of abutment surface contamination on screw loosening mechanisms in internal hexagonal implant connections. By analyzing mechanical changes under controlled *in vitro* cyclic loading conditions using statistical methods, this study aimed to clarify the clinical and mechanistic significance of abutment surface contamination on the mechanical stability of the implant-abutment joint. The null hypothesis was that the extent of abutment surface contamination within the internal hexagonal implant connection would not affect the mechanical stability of the implant-abutment joint under cyclic loading.

MATERIALS AND METHODS

From October 2021 to October 2022, all custom abutments delivered from external dental laboratories to the Department of Prosthodontics at a university hospital were examined under a stereomicroscope (SMZ-171; Motic, Xiamen, China) at ×20 magnification before clinical use. The presence of visible contaminants, such as stone particles, polishing residues, or unidentified debris, was documented on the abutment surface, particularly within the internal hexagonal connection area. Based on the extent of contamination, each abutment was classified into one of three categories: no contamination (N-CT), partial contamination (P-CT), and full contamination (F-CT), as summarized in Table 1.

Ninety titanium implants (Ø4.5 × 11.5 mm; Neo Biotech Co. Ltd., Seoul, Korea) were individually embedded in auto-polymerizing acrylic resin blocks (Ortho-Jet; Lang Dental Mfg. Co., Wheeling, IL, USA) in accordance with ISO 14801:2016 guidelines. After polymerization, prefabricated titanium abutments (Ø4.5 × 5.5 mm; Neobiotech Co., LTD., Seoul, Korea) were connected to each implant using titanium abutment screws (Ø1.5 × 13 mm; Neobiotech Co., LTD., Seoul, Korea).

Specimens were randomly assigned to three groups (n = 30 per group) according to the extent of contamination on the internal hexagonal connection surfaces (Fig. 2): CT0 (control), clean abutments without contamination; CT3 (moderate), contamination applied to three altering, non-adjacent internal hexagonal surfaces; and CT6 (severe), contamination applied to all six internal hexagonal surfaces. Contamination was simulated using a mixture of type III dental stone (Snow Rock Dental Stone; DK Mungyo, Gimhae, Korea) and distilled water, applied to the designated internal hexagonal surfaces with a microbrush by a single calibrated operator.

Abutment screws were tightened to 30 N·cm using a calibrated digital torque device (MGT-12; Mark-10 Corp, Copiague, NY, USA), followed by a 10-minute settling period and re-tightening to the same torque. Pre-loading reverse torque values (pre-RTVs) were measured 5 minutes after re-tightening. Specimens were then subjected to cyclic loading in accordance with ISO 14801:2016 (90 N, 2 Hz, 240,000 cycles). After loading, post-loading reverse torque values (post-RTVs) were measured using the same protocol (Fig. 3).

To qualitatively assess surface alterations after completion of the cyclic loading protocol (240,000 cycles), a subset of specimens from CT0 and CT6 was randomly selected. The specimens were sputter-coated with gold and examined under scanning electron microscopy (SEM; S-3000N, Hitachi, Krefeld, Germany). Images were acquired at magnifications of ×150, ×500, and ×2000.

The Shapiro-Wilk test was used to assess the normality of the data distribution within each group. To evaluate the effect of surface contamination and mechanical loading on preload maintenance, paired t-tests were employed to compare pre- and post-loading RTVs within each contamination group, and Bonferroni correction was applied to adjust for multiple comparisons. Differences in the absolute torque loss (ΔRTV) among the three groups were assessed using one-way analysis of variance (ANOVA), followed by Tukey's honestly significant difference (HSD) post hoc test to identify intergroup differences.

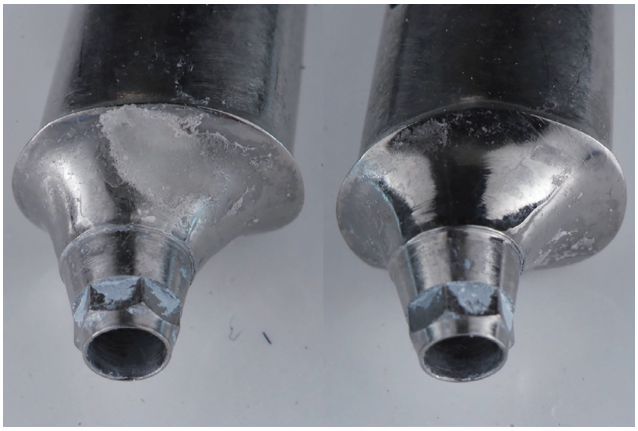

Fig. 1. Clinical photographs showing contamination on internal flat surfaces of hexagonal implant–abutment connection observed during routine clinical procedures.

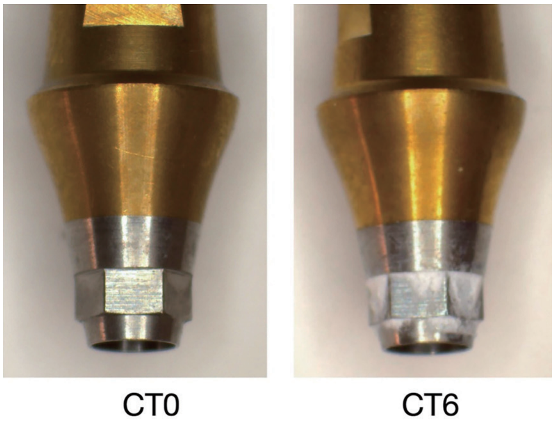

Fig. 2. Test group specimens with internal hexagonal implant–abutment connections contaminated with type III dental stone: CT0 (control) and CT6 (full contamination).

https://doi.org/10.4047/jap.2026.18.2.145

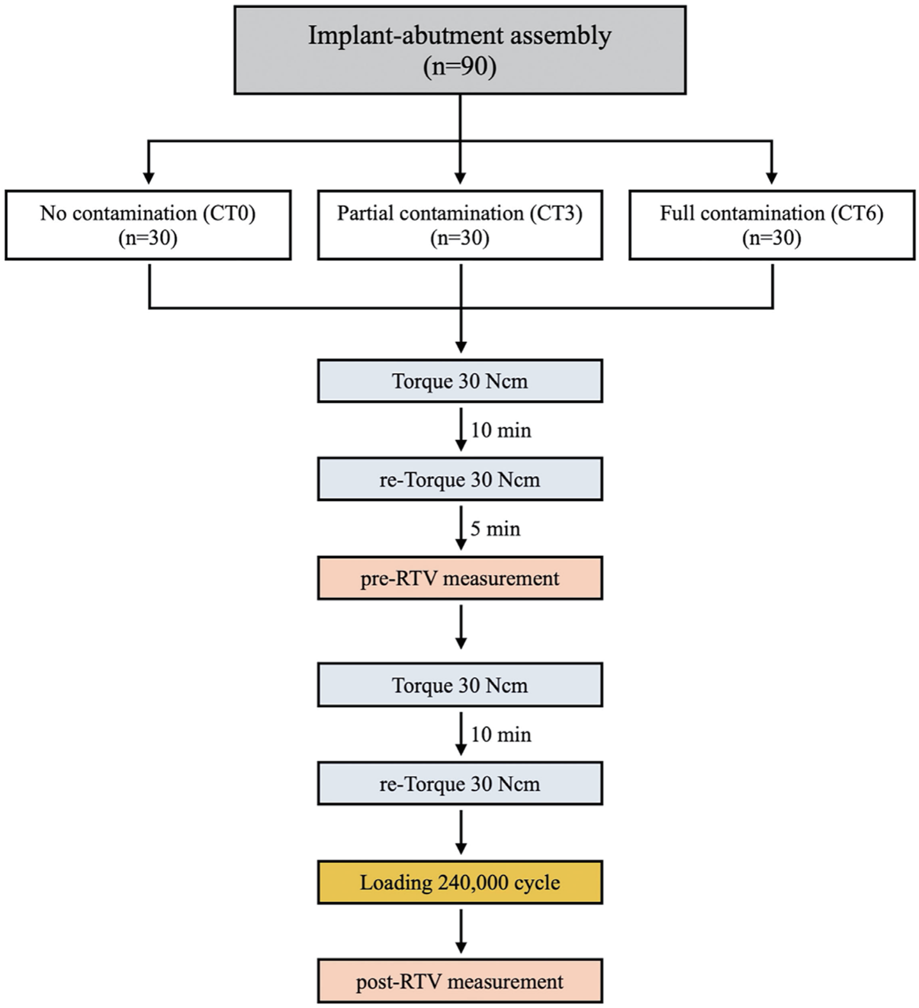

Fig. 3. Flow chart of experiment. RTV, reverse torque value.

Intergroup comparisons of pre- and post-loading RTV values were separately performed using one-way ANOVA with Tukey HSD post hoc analysis. All statistical analyses were performed by using a statistical software program (IBM SPSS Statistics, v29.0; IBM Corp., Armonk, NY, USA) ($\alpha = .05$).

RESULTS

A total of 265 custom abutments were evaluated upon delivery from external dental laboratories. Each abutment was inspected under ×20 magnification, and visible surface contamination was categorized into one of three groups. Overall, 29.06% of custom abutments exhibited detectable surface contamination, most commonly consisting of stone particles or polishing residues within the internal hexagonal connection surfaces (Table 1).

Table 1. Frequency of custom abutments assigned to each contamination group based on visual inspection upon delivery from external laboratories

	Number (N)	Percentage (%)
N-CT (No contamination)	188	70.94
P-CT (Partial Contamination)	65	24.53
F-CT (Full Contamination)	12	4.53
Total	265	100.00

Pre-RTVs differed significantly among the experimental groups ($P < .001$). The control group (CT0) demonstrated the highest pre-RTVs (27.9 ± 1.8 N·cm), which were significantly greater than those of both CT3 (23.2 ± 2.7 N·cm) and CT6 (22.9 ± 2.9 N·cm). No significant difference was observed between CT3 and CT6 (Table 2, Fig. 4).

After cyclic loading, post-RTVs also showed significant intergroup differences ($P < .001$). Post-RTVs decreased progressively with increasing contamination severity, with the highest values recorded in CT0 (21.5 ± 3.7 N·cm) and the lowest in CT6 (8.3 ± 4.7 N·cm) (Table 2, Fig. 4).

Analysis of absolute torque loss between pre- and post-loading conditions (ΔRTV) revealed significant differences among groups ($P < .001$). Torque loss was significantly greater in CT6 (14.6 ± 5.3 N·cm) than in CT0 (6.5 ± 3.8 N·cm; $P < .001$) and CT3 (8.6 ± 4.4 N·cm; $P < .001$). No significant difference in torque loss was observed between CT0 and CT3 (Table 2, Fig. 5).

Scanning electron microscopy (SEM) revealed minimal surface alteration in the uncontaminated control specimens, with only faint machining marks observed both before and after cyclic loading. In contrast, contaminated specimens demonstrated surface wear in the form of linear abrasion patterns predominantly located along the line angles (Fig. 6).

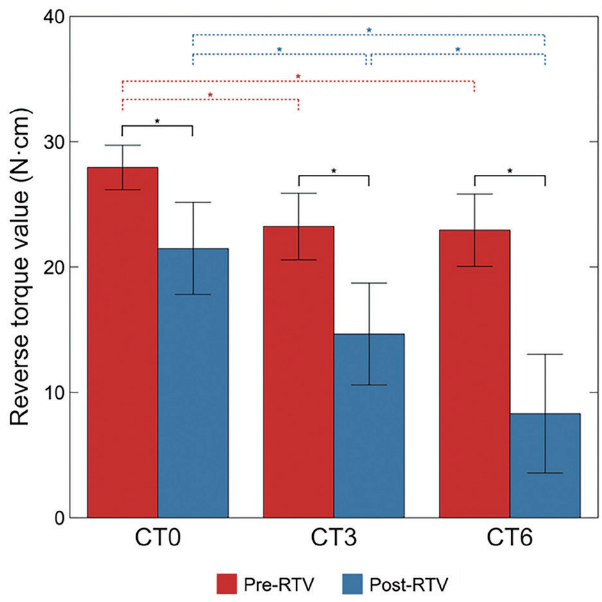

Fig. 4. Pre- and post-loading RTVs with significant differences (asterisks): black lines for within-group comparison, red lines for between-group pre-loading values, and blue lines for between-group post-loading values. Error bars represent standard deviations.
RTV, reverse torque value.

DISCUSSION

The present study quantitatively evaluated the effects of abutment contamination on implant-abutment joint stability in an internal hexagonal connection. The findings demonstrate that the mechanical influence of surface contamination is not governed by a single mechanism but manifests at two distinct mechanical stages: the formation of initial preload, reflected by preloading reverse torque values (pre-RTVs), and the dissipation of preload under functional loading, represented by changes in reverse torque after cyclic loading (ΔRTV). Accordingly, the null hypothesis was rejected.

Table 2. Pre- and post-loading RTVs, torque loss rates, and absolute torque loss (ΔRTV) for each contamination group

	pre-RTVs (Ncm)	pre-Torque loss rate (%)	post-RTVs (Ncm)	post-Torque loss rate (%)	ΔRTV (Ncm)	pre-post-Toruqe loss rate (%)
CT0 (control)	27.9 ± 1.8[a]	6.9	21.5 ± 3.7[a]	28.4	6.5 ± 3.8[a]	22.9
CT3 (moderate)	23.2 ± 2.7[b]	22.6	14.7 ± 4.1[b]	51.1	8.6 ± 4.4[a]	36.5
CT6 (severe)	22.9 ± 2.9[b]	22.5	8.3 ± 4.7[c]	72.3	14.6 ± 5.3[b]	63.5

Data are expressed as mean ± standard deviation. Different lowercase letters within same column indicate statistically significant differences.
RTV: reverse torque value.

https://doi.org/10.4047/jap.2026.18.2.145

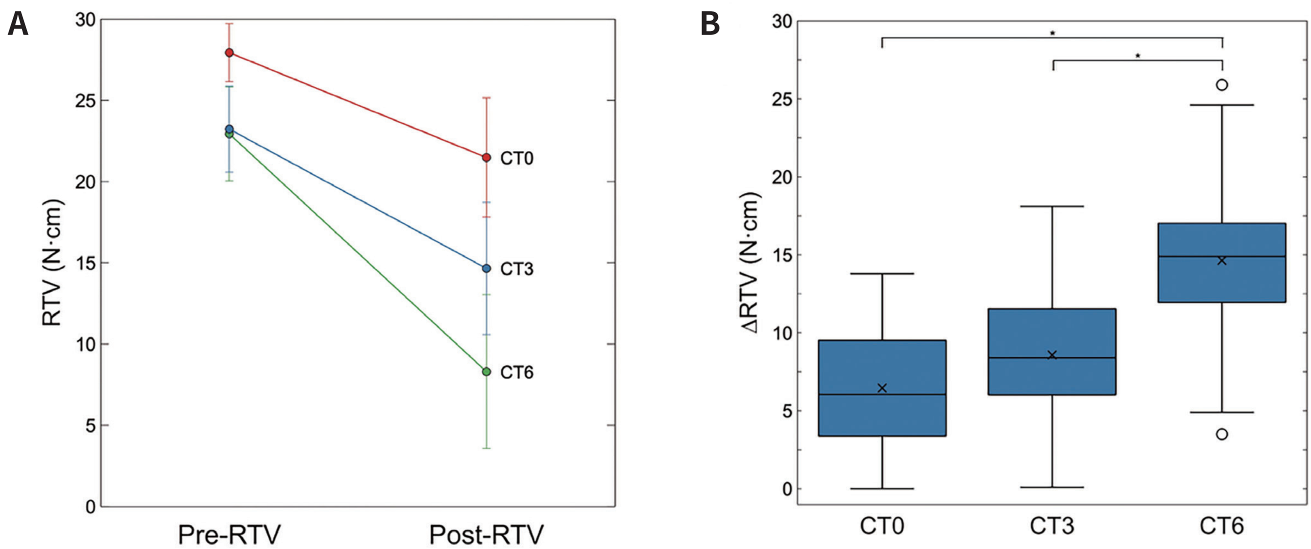

Fig. 5. (A) Comparison of RTV across groups, showing greater loss from pre- to post-loading with increasing contamination severity. (B) Box plot of preload loss (ΔRTV) after cyclic loading. Asterisks indicate significant differences between groups. RTV, reverse torque value.

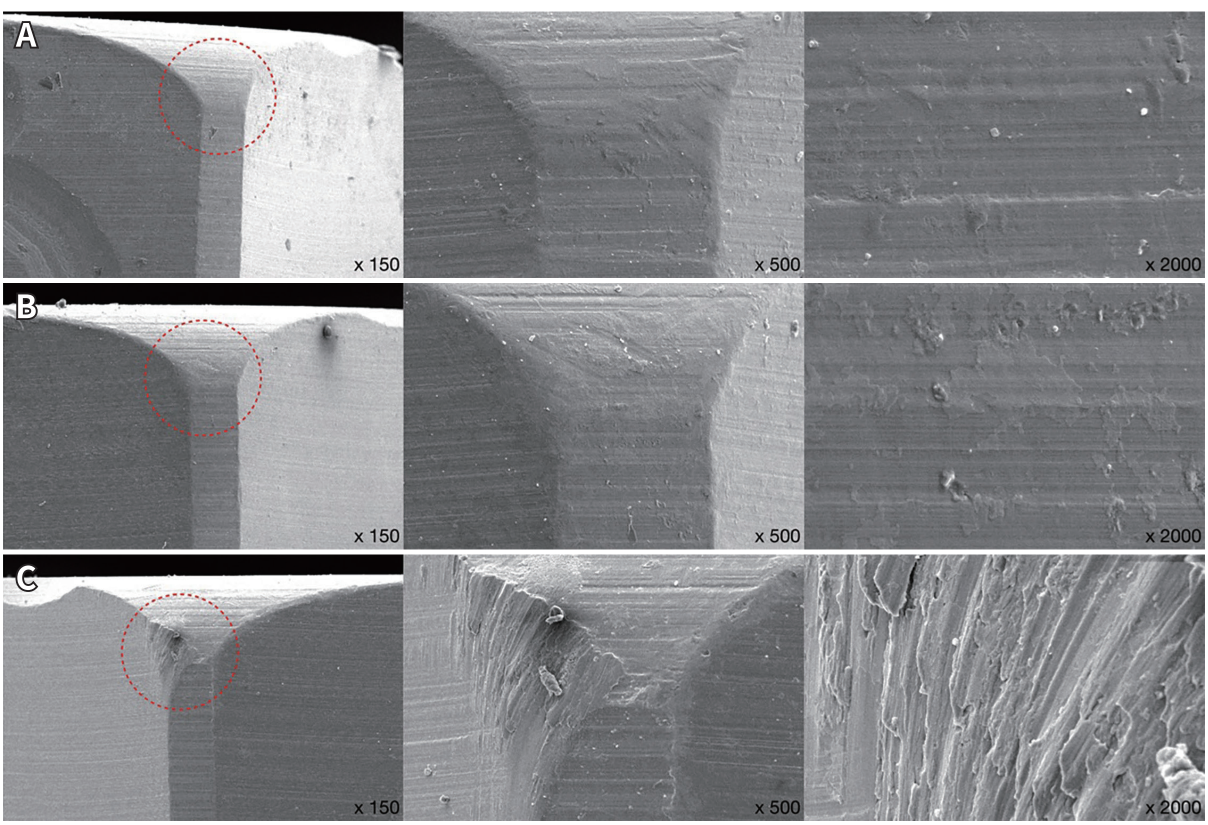

Fig. 6. Representative SEM images of internal hexagonal connection under different conditions. (A) CT0 before cyclic loading; (B) CT0 after cyclic loading, exhibiting minimal additional wear consistent with baseline surface changes; (C) CT6 after cyclic loading, abrasion in line angles, where contact with implant is concentrated. Images in each row are shown at ×150, ×500, and ×2000 magnification from left to right. SEM, scanning electron microscope.

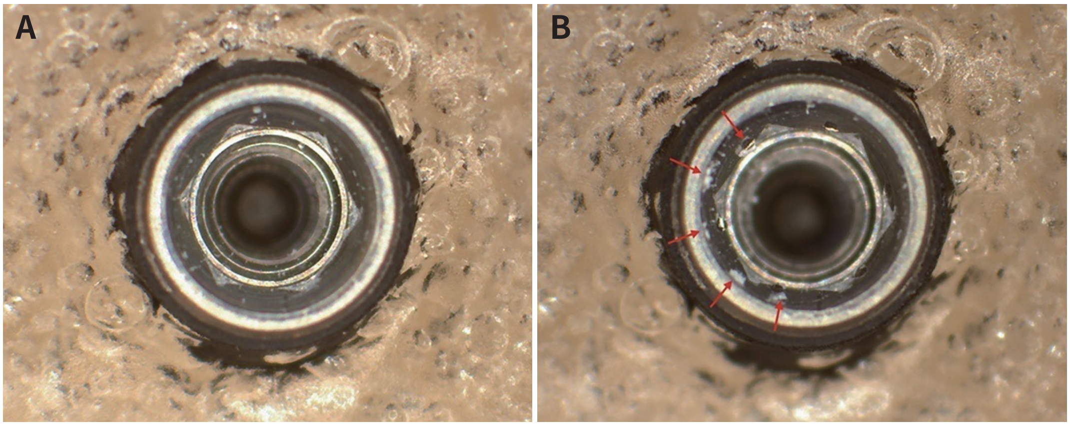

Fig. 7. Stereomicroscopic images of internal wall of implant fixture before and after seating contaminated abutment. (A) Before abutment connection, showing clean internal surface; (B) After connection and removal of contaminated abutment, debris (red arrows) is visible along internal wall, demonstrating transfer of contamination into fixture.

The significantly reduced pre-RTVs observed in both contaminated groups (CT3 and CT6) suggest that surface contamination compromises conversion of tightening torque into effective preload. Because preload establishment depends on complete seating and intimate contact between surfaces, contamination within the internal connection likely interferes with full abutment seating, thereby limiting the achievable clamping force at the time of initial tightening. This observation is consistent with previous *in vitro* findings demonstrating that interfacial contamination or tissue entrapment can impede complete seating and reduce effective preload generation during initial tightening.[11] Notably, no significant difference in pre-RTVs was detected between CT3 and CT6, suggesting that even a limited amount of contamination may be sufficient to disrupt initial preload formation, regardless of its extent.

In contrast, analysis of absolute torque loss (ΔRTV) after cyclic loading revealed a different pattern. ΔRTV reflects not only the magnitude of torque reduction but also the behavior of preload dissipation under functional loading. The significantly greater ΔRTV observed in CT6 indicates that extensive contamination accelerates preload loss during cyclic loading. Conversely, although CT3 demonstrated reduced initial preload, its preload dissipation pattern under cyclic loading was comparable to that of the uncontaminated control group. These findings imply that the pattern of preload dissipation under functional loading varies according to the extent of contamination.

Taken together, abutment contamination produced a distinct pattern of mechanical behavior at the implant-abutment interface. The control group exhibited both efficient preload formation and stable preload maintenance. The partially contaminated group (CT3) showed compromised initial preload formation but relatively preserved preload stability pattern under cyclic loading. In contrast, the extensively contaminated group (CT6) demonstrated both compromised initial preload formation and preload maintenance.

Previous studies on abutment screw loosening have primarily explained the underlying mechanical mechanisms by focusing on the relationship between tightening torque and preload, the coefficient of friction at the contacting surfaces, the settling effect occurring immediately after tightening, and micromotion and surface wear induced by cyclic loading.[14,24-31] In particular, Bickford has described screw loosening as a continuous and unified mechanical process, in which reduced preload leads to increased micromotion, followed by localized wear and progressive torque loss.[17] In many *in vitro* investigations, variables such as contamination, lubrication, or surface coating have

https://doi.org/10.4047/jap.2026.18.2.145

been evaluated using a single outcome measure, most commonly preload reduction or reverse torque loss.

Consequently, preload formation and preload maintenance or dissipation have generally been interpreted along the same linear mechanistic pathway. In contrast, the findings of the present study indicate that preload behavior is governed by distinct mechanisms at different stages. The early conversion of tightening torque into preload was sensitive to the mere presence of contamination, whereas preload dissipation under cyclic loading demonstrated extent-dependent behavior. Accordingly, the present findings support a stepwise reinterpretation of screw loosening mechanisms that have traditionally regarded preload loss as a unified outcome.

The observed mechanical behavior may be explained by the interaction between residual contaminants and the internal hexagonal connection geometry. Particulate contamination within the connection can prevent complete seating of the abutment, resulting in reduced initial clamping force and increased susceptibility to micromotion under functional loading.[17] Under cyclic loading, contaminants specifically located in the line angle and localized contact regions may contribute to stress concentration and progressive surface wear. This mechanism is supported by scanning electron microscopy (SEM) findings, which demonstrated localized linear abrasion patterns along line angles in contaminated specimens (Fig. 6), whereas uncontaminated specimens exhibited barely detectable machining marks. Such localized wear and microgap enlargement may further diminish antirotational stability and accelerate preload loss over time.

An important clinical implication of these findings relates to the internal flat surfaces of hexagonal abutment connections. Despite the planar nature of these surfaces, contamination may be difficult to detect without magnification, particularly when contamination is minimal. As a result, contamination may be overlooked during clinical try-in procedures. If contaminated abutments are inserted without prior detection, contaminants are transferred into the internal aspect of the implant fixture, where subsequent access and removal become more challenging (Fig. 7). Once contaminants are introduced into the fixture, repeated tightening may remain compromised by incomplete seating, potentially perpetuating preload instability. From a clinical perspective, the primary risk lies not in the technical difficulty of cleaning, but in delayed or missed recognition of contamination.

Unlike prefabricated abutments, custom abutments undergo multiple fabrication steps, including milling, finishing, and polishing, during which surface contamination may occur. This risk may be further increased when abutments are manufactured by external dental laboratories, where process standardization and contamination control can be variable. Although surface contamination may appear clinically insignificant, the present findings suggest that it can directly compromise implant-abutment joint stability. Accordingly, careful inspection and decontamination of custom abutments before clinical insertion should be considered an essential step in implant prosthodontic procedures.

Several limitations of this study should be acknowledged. The investigation was conducted under *in vitro* conditions and therefore did not fully reproduce the complex biological environment of the oral cavity. In addition, a single type of particulate contamination was evaluated, which may not represent the full spectrum of contaminants encountered clinically. Furthermore, the analysis was limited to internal hexagonal connections, and generalization of these findings to other connection designs should be performed with caution. Future studies incorporating different contamination types, connection geometries, repeated tightening protocols, and extended loading durations are warranted to further elucidate the clinical relevance of surface contamination on implant-abutment stability.

CONCLUSION

Surface contamination within an internal hexagonal implant-abutment connection adversely affects joint stability through two distinct mechanical stages. While the presence of contamination primarily compromises initial preload formation, extensive contamination accelerates preload loss under cyclic loading. These findings suggest that even subtle contamination, often overlooked clinically, may have meaningful implications for implant-abutment stability.

REFERENCES

1. Goodacre CJ, Bernal G, Rungcharassaeng K, Kan JY. Clinical complications with implants and implant prostheses. J Prosthet Dent 2003;90:121-32.
2. Pjetursson BE, Asgeirsson AG, Zwahlen M, Sailer I. Improvements in implant dentistry over the last decade: comparison of survival and complication rates in older and newer publications. Int J Oral Maxillofac Implants 2014;29 Suppl:308-24.
3. Howe MS, Keys W, Richards D. Long-term (10-year) dental implant survival: a systematic review and sensitivity meta-analysis. J Dent 2019;84:9-21.
4. Fu JH, Hsu YT, Wang HL. Identifying occlusal overload and how to deal with it to avoid marginal bone loss around implants. Eur J Oral Implantol 2012;5 Suppl:S91-103.
5. Xia D, Lin H, Yuan S, Bai W, Zheng G. Dynamic fatigue performance of implant-abutment assemblies with different tightening torque values. Biomed Mater Eng 2014;24:2143-9.
6. Broggini N, McManus LM, Hermann JS, Medina RU, Oates TW, Schenk RK, Buser D, Mellonig JT, Cochran DL. Persistent acute inflammation at the implant-abutment interface. J Dent Res 2003;82:232-7.
7. Park IS, Won SY, Bae TS, Song KY, Park CW, Eom TG, Jeong CM. Fatigue characteristics of five types of implant-abutment joint designs. Met Mater Int 2008;14:133-8.
8. Chae SW, Kim YS, Lee YM, Kim WK, Lee YK, Kim SH. Complication incidence of two implant systems up to six years: a comparison between internal and external connection implants. J Periodontal Implant Sci 2015;45:23-9.
9. Vetromilla BM, Brondani LP, Pereira-Cenci T, Bergoli CD. Influence of different implant-abutment connection designs on the mechanical and biological behavior of single-tooth implants in the maxillary esthetic zone: a systematic review. J Prosthet Dent 2019;121:398-403.e3.
10. Vigolo P, Gracis S, Carboncini F, Mutinelli S; AIOP (Italian Academy of Prosthetic Dentistry) Clinical Research Group. Internal- vs external-connection single implants: a retrospective study in an italian population treated by certified prosthodontists. Int J Oral Maxillofac Implants 2016;31:1385-96.
11. Zeno HA, Buitrago RL, Sternberger SS, Patt ME, Tovar N, Coelho P, Kurtz KS, Tuminelli FJ. The effect of tissue entrapment on screw loosening at the implant/abutment interface of external- and internal-connection implants: an in vitro study. J Prosthodont 2016;25:216-23.
12. Dhingra A, Weiner S, Luke AC, Ricci JL. Analysis of dimensional changes in the screw and the surface topography at the interface of a titanium screw and a zirconia abutment under cyclic loading: an in vitro study. Int J Oral Maxillofac Implants 2013;28:661-9.
13. Jo JY, Yang DS, Huh JB, Heo JC, Yun MJ, Jeong CM. Influence of abutment materials on the implant-abutment joint stability in internal conical connection type implant systems. J Adv Prosthodont 2014;6:491-7.
14. Lee JH, Cha HS. Screw loosening and changes in removal torque relative to abutment screw length in a dental implant with external abutment connection after oblique cyclic loading. J Adv Prosthodont 2018;10:415-21.
15. Shinohara R, Ueda K, Watanabe F. Influence of the difference between implant body and screw materials on abutment screw loosening. Dent Mater J 2019;38:150-6.
16. Ganapathy DM. Effect of coated surfaces influencing screw loosening in implants: a systematic review and meta-analysis. World J Dent 2017;8:496-502.
17. Bickford JH, Oliver M. Introduction to the design and behavior of bolted Joints. 5th ed. CRC Press; 2022. p. 520-42.
18. Lee HW, Alkumru H, Ganss B, Lai JY, Ramp LC, Liu PR. The effect of contamination of implant screws on reverse torque. Int J Oral Maxillofac Implants 2015;30:1054-60.
19. Sun F, Cheng W, Zhao BH, Song GQ, Lin Z. Evaluation the loosening of abutment screws in fluid contamination: an in vitro study. Sci Rep 2022;12:10797.
20. Bulaqi HA, Barzegar A, Paknejad M, Safari H. Assessment of preload, remaining torque, and removal torque in abutment screws under different frictional

 https://doi.org/10.4047/jap.2026.18.2.145

conditions: A finite element analysis. J Prosthet Dent 2019;121:548.e1-7.
21. Canullo L, Micarelli C, Iannello G. Microscopical and chemical surface characterization of the gingival portion and connection of an internal hexagon abutment before and after different technical stages of preparation. Clin Oral Implants Res 2013;24:606-11.
22. Kim S, Choi C, Cha Y, Chang JS. The efficacy of convenient cleaning methods applicable for customized abutments: an in vitro study. BMC Oral Health 2021;21:78.
23. Gehrke P, Abazari C, Schlichter K, Fischer C, Duddeck D, Romanos GE, Weigl P. Qualitative and semi-quantitative assessment of processing-related surface contamination of one- and two-piece CAD/CAM abutments before and after ultrasonic cleaning. Materials (Basel) 2020;13:3225.
24. McGlumphy EA, Mendel DA, Holloway JA. Implant screw mechanics. Dent Clin North Am 1998;42:71-89.
25. Siamos G, Winkler S, Boberick KG. Relationship between implant preload and screw loosening on implant-supported prostheses. J Oral Implantol 2002;28:67-73.
26. Martin WC, Woody RD, Miller BH, Miller AW. Implant abutment screw rotations and preloads for four different screw materials and surfaces. J Prosthet Dent 2001;86:24-32.
27. Wentaschek S, Tomalla S, Schmidtmann I, Lehmann KM. Preload, coefficient of friction, and thread friction in an implant-abutment-screw complex. Int J Prosthodont 2017;30:542-4.
28. Sagheb K, Görgen CI, Döll S, Schmidtmann I, Wentaschek S. Preload and friction in an implant-abutment-screw complex including a carbon-coated titanium alloy abutment screw: an in vitro study. Int J Implant Dent 2023;9:8.
29. Winkler S, Ring K, Ring JD, Boberick KG. Implant screw mechanics and the settling effect: overview. J Oral Implantol 2003;29:242-5.
30. Cantwell A, Hobkirk JA. Preload loss in gold prosthesis-retaining screws as a function of time. Int J Oral Maxillofac Implants 2004;19:124-32.
31. Gratton DG, Aquilino SA, Stanford CM. Micromotion and dynamic fatigue properties of the dental implant-abutment interface. J Prosthet Dent 2001;85:47-52.